

## Effect of UV/ozone treatment on the wettability and adhesion of polymeric systems

Hamdi, Marouen; Poulis, Johannes A.

**DOI**

[10.1080/00218464.2019.1693372](https://doi.org/10.1080/00218464.2019.1693372)

**Publication date**

2019

**Document Version**

Final published version

**Published in**

Journal of Adhesion

**Citation (APA)**

Hamdi, M., & Poulis, J. A. (2019). Effect of UV/ozone treatment on the wettability and adhesion of polymeric systems. *Journal of Adhesion*, 97(7), 651-671. Advance online publication. <https://doi.org/10.1080/00218464.2019.1693372>

**Important note**

To cite this publication, please use the final published version (if applicable). Please check the document version above.

**Copyright**

Other than for strictly personal use, it is not permitted to download, forward or distribute the text or part of it, without the consent of the author(s) and/or copyright holder(s), unless the work is under an open content license such as Creative Commons.

**Takedown policy**

Please contact us and provide details if you believe this document breaches copyrights. We will remove access to the work immediately and investigate your claim.

***Green Open Access added to TU Delft Institutional Repository***

***'You share, we take care!' - Taverne project***

**<https://www.openaccess.nl/en/you-share-we-take-care>**

Otherwise as indicated in the copyright section: the publisher is the copyright holder of this work and the author uses the Dutch legislation to make this work public.



## Effect of UV/ozone treatment on the wettability and adhesion of polymeric systems

Marouen Hamdi & Johannes A. Poulis

To cite this article: Marouen Hamdi & Johannes A. Poulis (2019): Effect of UV/ozone treatment on the wettability and adhesion of polymeric systems, The Journal of Adhesion, DOI: [10.1080/00218464.2019.1693372](https://doi.org/10.1080/00218464.2019.1693372)

To link to this article: <https://doi.org/10.1080/00218464.2019.1693372>



Published online: 20 Nov 2019.



Submit your article to this journal [↗](#)



Article views: 25





View related articles [↗](#)



View Crossmark data [↗](#)



# Effect of UV/ozone treatment on the wettability and adhesion of polymeric systems

Marouen Hamdi  and Johannes A. Poulis 

Structural Integrity and Composites (SI&C) Group, Department of Aerospace Structures and Materials, Faculty of Aerospace Engineering, Delft University of Technology, Delft, The Netherlands

## ABSTRACT

The impact of UV/ozone treatment on the wettability and adhesion of ethylene propylene diene methylene (EPDM) rubber, polyvinyl chloride (PVC), and acrylonitrile butadiene styrene (ABS) was investigated using contact angle measurements, OWRK surface free energy model, standardized adhesion tests, and spectroscopic and microscopic observations. It is found that UV/ozone treatment enhances the wettability of the examined polymers. Also, it considerably improved the adhesion strength of PVC and ABS samples, and shifted their failure modes from adhesive to cohesive. FTIR-ATR characterization showed insignificant changes in the chemical structures of the studied materials. However, SEM observation showed newly-created wrinkles and micro-holes on treated PVC surfaces, and micropores on ABS surfaces. These UV-induced morphological changes on PVC and ABS surfaces increased the surface area which can promote the mechanical interlocking with the adhesive. This explains the improvement of their adhesion strength. Implications of the current study for the processing of strongly bonded polymeric joints are discussed.

## ARTICLE HISTORY

Received 28 August 2019  
Accepted 12 November 2019

## KEYWORDS

UV/ozone treatment;  
wettability; adhesion; EPDM;  
PVC; ABS

## 1. Introduction

Polymeric materials are increasingly used in a wide variety of industrial applications. More and more attention is paid to these materials, which is reflected by extensive studies investigating their performance.<sup>[1,2]</sup> This is due to a range of attractive properties including their low cost, light weight, high processability, and significant chemical resistance. However, one of the major limitations of polymers is their low adhesion strength and wettability.<sup>[3]</sup> This is mainly due to their weak boundary layers induced by different factors such as the impurities arising during the polymerization process, polymer tails with a low molecular weight, additives (e.g., antioxidants, slip agents), external processing conditions (e.g., mould release agents), and post-processing contamination.<sup>[4]</sup> This limited adhesion strength hinders many large-scale industries, such as the automotive and aerospace industries, from benefiting from their full potential.

**CONTACT** Marouen Hamdi  [m.hamdi@tudelft.nl](mailto:m.hamdi@tudelft.nl)  Faculty of Aerospace Engineering, Department of Aerospace Structures and Materials, Group of Structural Integrity and Composites, Delft University of Technology, Kluyverweg 1, 2629, HS Delft, The Netherlands

Color versions of one or more of the figures in the article can be found online at [www.tandfonline.com/gadh](http://www.tandfonline.com/gadh).

To improve their adhesion performance, polymeric materials and composites are usually subjected to different surface treatments such as corona, glow charge, and abrasion treatments.<sup>[5]</sup> One of the common treatments is atmospheric pressure plasma torch (APPT), extensively investigated by Encinas and co-workers.<sup>[6–10]</sup> These studies found that the adhesion strength of polypropylene (PP) and silicone surfaces increased after APPT treatment.<sup>[6,9]</sup> Another widely used surface treatment is UV/ozone treatment.<sup>[11]</sup> In this treatment, the produced photons have sufficient energy to break most C – C bonds and trigger chain scission and crosslinking mechanisms on the polymeric surface.<sup>[12]</sup> Thus, this treatment is chemical, by creating new functional groups on the surface, but also topographical, by removing the upper cohesively weak-bonded layers.<sup>[3]</sup> It is argued that the topographical function of UV/ozone treatment is the essential one and its chemical function is just secondary.<sup>[4]</sup> The efficiency of UV/ozone treatment depends on the physical and mechanical properties of each polymer. For instance, a previous study found that the bonding strength of polyethylene (PE) increased consistently after UV/ozone treatment, while that of polyetheretherketone (PEEK) initially increased after 2 min of treatment then decreased.<sup>[3]</sup> This was explained by the chain scission damage mechanism of PEEK structure at higher durations of UV irradiation. Also, the treatment effect depends on the experimental conditions such as the source-sample distance, treatment duration, UV lamp power and wavelength, and oxygen/ozone concentration.<sup>[13]</sup>

The adhesion strength is usually associated with the surface wettability, which is a crucial property for many industrial applications such as cleaning, coating, and painting.<sup>[14]</sup> Previous studies investigated the effect of different parameters on the wettability of polymers. For example, it is found that Teflon wettability increased with higher surface roughness, changed mechanically using grit blasting or chemically using NaOH and HNO<sub>3</sub>/KMnO<sub>4</sub> solutions.<sup>[15,16]</sup> This was not the case for plasma polymer thin films (pp-GT) and Na-treated Teflon.<sup>[15,17]</sup> Therefore, a correlation cannot be made between surface wettability and roughness. Also, the wettability can be changed through other surface treatments. For instance, previous studies showed that atmospheric pressure plasma torch (APPT) treatment significantly improved the wettability of high-density polyethylene (HDPE), low-density polyethylene (LDPE), polypropylene (PP), and acrylonitrile butadiene styrene (ABS) by increasing the surface oxygen content and decreasing the carbon content.<sup>[6,7,18]</sup>

To determine the wettability of polymers, several models were developed such as Owens–Wendt–Rabel–Kaelbe (OWRK)<sup>[19,20]</sup>, Fowkes<sup>[14,21]</sup>, Zisman<sup>[22,23]</sup>, van Oss<sup>[24]</sup>, equation of state (EOS)<sup>[25]</sup>, and Wu<sup>[14,21,26]</sup> models. Each of these models is recommended for particular types of materials depending on their surface properties (e.g., polarity, etc.). OWRK model is the most commonly used model because it allows the generation of the *wetting envelopes* based on contact angle measurements.<sup>[14,17,21]</sup> The major advantage of these envelopes is determining the wettability of other solvents with known polar and disperse surface

tension components. This is highly beneficial in the selection of the appropriate solvents, lubricants, sealants, and adhesives for particular materials.<sup>[15]</sup>

In this study, the impact of UV/ozone treatment on the wettability and adhesion behavior of widely used polymeric systems is investigated. The wetting envelopes of the studied materials were generated using OWRK model. The usefulness of this treatment in the processing of polymeric surfaces with enhanced wettability and adhesion properties is discussed.

## **2. Experimental**

### **2.1. Model systems**

The model systems examined in this study consist of commercialized ethylene propylene diene methylene (EPDM) rubber, polyvinyl chloride (PVC), and acrylonitrile butadiene styrene (ABS) with thickness values of 1.1 mm, 1.2 mm, and 4 mm, respectively. They were provided by Vink Kunststoffen (Netherlands), Firestone Building Products (USA), and Royal Roofing Materials (Netherlands) companies, consecutively. Flexible EPDM and PVC materials are commonly used as roofing materials. Hard ABS material is an impact-modified styrenic polymer which usually contains light stabilizers and antioxidants to reduce its susceptibility to ultraviolet (UV) radiation.<sup>[27]</sup>

### **2.2. UV/ozone treatment**

To perform the UV/ozone treatment, the samples were first cleaned according to ASTM D2093 standard.<sup>[28]</sup> Then, they were isolated in a closed box and exposed to UV light in combination with ozone gas for 3, 5, 7, and 10 min at room temperature. Only ambient air was used and no oxygen concentrator, fan, or air pump was employed. The box is equipped with three ozone-generating UV disinfection lamps with a power of 35 W each, emitting UV light with a wavelength range of 185.49–253.742 nm. The distance between the samples and the UV lamps is about 35 mm.

### **2.3. Contact angle measurements**

Static contact angles were measured using a KSV Instrument CAM 200 system (Biolin Scientific, Helsinki, Finland) based on the sessile drop method. For each material, measurements were taken at room temperature from different samples and locations (center and edges) to obtain representative results. Four solvents, namely, water, ethylene glycol-water (1:1), glycerol, and ethyl acetate were used to determine the surface energy. The polar and dispersive components of their surface tensions are presented in [Table 1](#).

**Table 1.** Polar ( $\gamma_{lv}^p$ ) and dispersive ( $\gamma_{lv}^d$ ) components of the surface tension ( $\gamma_{lv}$ ) of the solvents at 20°C (mN.m<sup>-1</sup>).

Solvent	$\gamma_{lv}$	$\gamma_{lv}^p$	$\gamma_{lv}^d$	Refs.
Water	72.8	51	21.8	[20]
Ethylene glycol-water (1:1)	57.9	37.9	20	[29]
Glycerol	63.4	22.8	40.6	[30]
Ethyl Acetate	23.9	0	23.9	[31]

## 2.4. Adhesion tests

The bonded joints were prepared using a one-component adhesive provided by Henkel Corporation (Düsseldorf, Germany). It consists in a silane-modified (MS) polymer with a moisture-curing process. Its physical and mechanical properties are presented in Table 2. First, the adhesives were mixed with 1 wt% of glass beads provided by Sigma Aldrich (St. Louis, USA) with diameter in the range between 212  $\mu\text{m}$  and 300  $\mu\text{m}$ . This technique is commonly used to maintain a uniform and consistent thickness across the bond-line without affecting the adhesive properties.<sup>[5,32–34]</sup> Then, the adhesives were applied on the model systems using a curing schedule of approximately 1 week at room temperature.

To determine the adhesion strength of the flexible EPDM and PVC samples, T-peel tests were conducted according to ASTM D1876 standard at a crosshead speed of 254 mm/min.<sup>[35]</sup> Similarly, lap-shear tests were performed on rigid ABS samples according to ASTM D3163 standard at a crosshead speed of 1.27 mm/min.<sup>[36]</sup> These tests were executed using a Zwick Roell (Ulm, Germany) tensile test instrument with a maximum test load of 250 kN, coupled with a load cell of 10 kN.

## 2.5. FTIR-ATR characterization

Fourier-Transform Infrared Attenuated Total Reflectance (FTIR-ATR) characterization was performed to determine the effect of UV/ozone treatment on the chemical structure of the treated surfaces.<sup>[37]</sup> Spectra were acquired using a single-beam FT100 spectrometer in conjunction with an ATR accessory, manufactured by PerkinElmer (Waltham, USA). The instrument is equipped with a MIR TGS detector and a diamond/ZnSe crystal. Before conducting the tests, the samples

**Table 2.** Properties of the applied adhesive.

Chemical base	Silane-modified polymer
Curing process	Moisture curing
Density (g/cm <sup>3</sup> )	1.5
Tensile strength (ISO 37) (MPa)	3
Elongation at break (ISO 37) (%)	250
Shore-A-hardness (ISO 868)	55
Application temperature (°C)	5–40
In-service temperature (°C)	– 40 to 100

were first cleaned from any adhering particles. Then, IR spectra were collected as the changes in absorption within the range of 650–4000  $\text{cm}^{-1}$  at ambient conditions and a resolution of 4  $\text{cm}^{-1}$ , a data interval of 1  $\text{cm}^{-1}$ , a scan speed of 0.2  $\text{cm/s}$ , and a minimum of 30 scans. The collected data were then pre-processed by performing baseline and offset correction, and spectra normalization based on min-max method.<sup>[38]</sup>

## 2.6. Scanning electron microscopy (SEM)

To determine the effect of UV/ozone treatment on the morphological features of the studied materials, micrographs of untreated and treated surfaces were obtained using a JOEL JSM – 7500F microscope (Tokyo, JAPAN). The SEM images were acquired at an accelerating voltage of 5 kV and a probe current of approximately 10  $\mu\text{A}$ . The samples were first sputter-coated with gold for 90 s at a working pressure of  $10^{-4}$  mbar.

## 3. Results and discussion

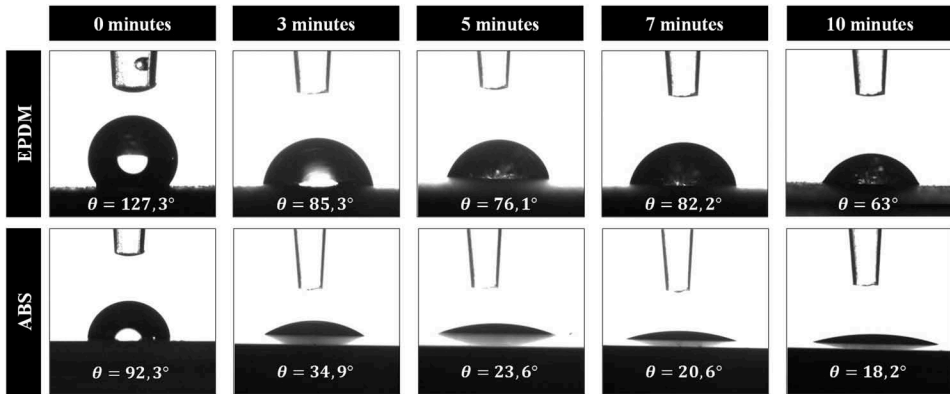
### 3.1. Wettability analysis

#### 3.1.1. Contact angle measurements

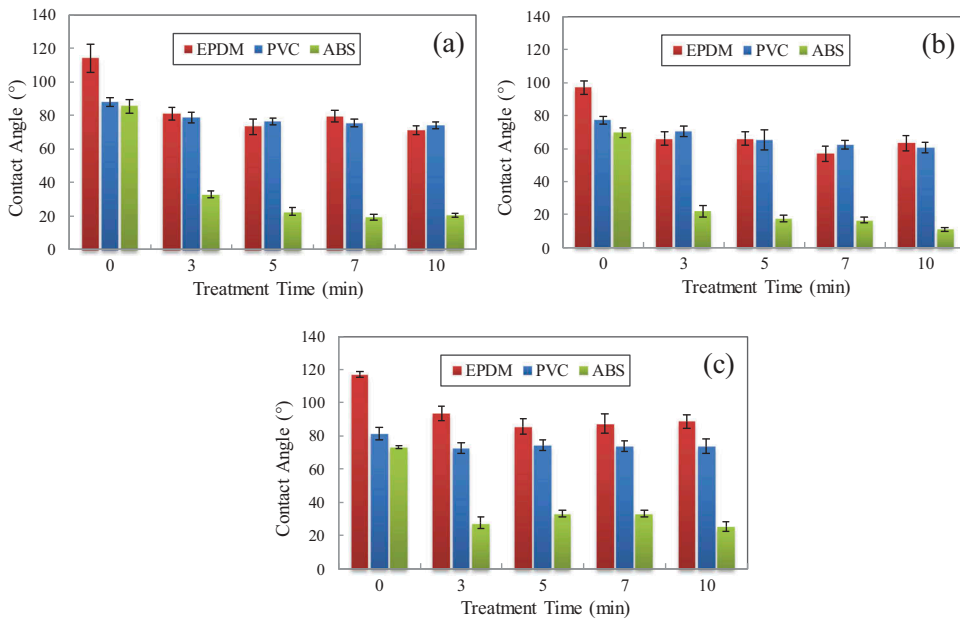
Figure 1 shows water drops deposited on EPDM and ABS surfaces and the corresponding contact angles for different durations of UV/ozone treatment. It is clearly visible that the contact angles decrease after treating the samples. This decrease is important after 3 min of treatment but less significant for higher durations. For instance, the contact angle of ABS went from 92.3° to 34.9° after 3 min, to only 23.7° after 5 min of treatment. Similar results were obtained using ethylene glycol-water and glycerol solvents. As for ethyl acetate, it was consistently used for ABS samples but quickly evaporated on treated EPDM and PVC surfaces. It is known that ethyl acetate has a low boiling point and a high evaporation rates.<sup>[39]</sup> The sudden evaporation of this solvent from flexible EPDM and PVC surfaces might be caused by the increase of their surface temperatures due to the heat generated by the UV lamps. This solvent did not evaporate on rigid ABS surfaces probably due to their lower UV-induced temperature. Similar observations were previously made in the literature for other solvents.<sup>[40]</sup> Thus, the results of ethyl acetate solvent will be considered only for ABS samples.

Figure 2 presents the contact angle measurements of the model systems using water, ethylene glycol-water, and glycerol. Figure 2a shows that the contact angle of water on untreated PVC is 85.4°. This result is consistent with a previous study that found an angle of 87°. <sup>[19]</sup> The figure clearly shows that the contact angles of EPDM and ABS decreased significantly after 3 min of UV/ozone treatment. For instance, glycerol measurements show that they went from 118.8° and 73.3° to 93.5° and 27.7°, respectively (Figure 2c). No





**Figure 1.** Water drops and contact angles on EPDM and ABS surfaces for different durations of UV/ozone treatment.



**Figure 2.** Contact angle measurements for different durations of UV/ozone treatment using (a) water, (b) ethylene glycol-water (1:1), and (c) glycerol.

significant changes are observed for higher treatment times. As for PVC, only a slight decrease is shown after treatment. Similar results were obtained for the other solvents, which shows the consistency of the measurements.

### 3.1.2. Owens–Wendt–Rabel–Kaelbe (OWRK) model

We consider first presenting the theoretical background of OWRK model. The thermodynamic wetting between a liquid and a solid is given by Young equation as follows<sup>[19]</sup>:

$$\gamma_{lv} \cos \theta = \gamma_{sv} - \gamma_{sl} - \pi_e \quad (1)$$

where  $\gamma_{lv}$ ,  $\gamma_{sv}$ , and  $\gamma_{sl}$  are, respectively, the free energies of the liquid against the saturated vapor, the solid against the saturated vapor, and the liquid-solid interface. The variables  $\theta$  and  $\pi_e$  are the contact angle and the equilibrium pressure of adsorbed vapor of the liquid on the solid, consecutively. This equation was used by Fowkes who assumed that:

$$\pi_e = 0 \text{ and } \gamma_{sl} = \gamma_{sv} + \gamma_{lv} - 2\sqrt{\gamma_s^d \gamma_l^d} \quad (2)$$

where  $\gamma_s^d$  and  $\gamma_l^d$  are the dispersive components of  $\gamma_{sv}$  and  $\gamma_{lv}$ . He derived the following expression of the contact angle of a liquid on a solid in terms of the contributions of their dispersive forces:

$$1 + \cos \theta = 2 \left( \frac{\sqrt{\gamma_l^d}}{\gamma_{lv}} \right) \sqrt{\gamma_s^d} \quad (3)$$

Furthermore, Owens and Wendt showed that the SFE can be divided into two components:  $\gamma^d$  representing the dispersion forces and  $\gamma^p$  representing the polar (intermolecular) interactions (i.e., dipole-dipole, hydrogen,  $\pi$ -bonding).<sup>[19]</sup>:

$$\gamma = \gamma^d + \gamma^p \quad (4)$$

Based on this approach and using Fowkes relation, OWRK model was developed initially for polymers.<sup>[19,20]</sup> It consists of introducing a linear relationship that allows the determination of the polar and dispersive components of the SFE of a solid<sup>[19,20]</sup>:

$$\frac{\gamma_{lv}(1 + \cos \theta)}{2\sqrt{\gamma_{lv}^d}} = \sqrt{\gamma_s^p} \sqrt{\frac{\gamma_{lv}^p}{\gamma_{lv}^d}} + \sqrt{\gamma_s^d} \quad (5)$$

where  $\gamma_{lv}^p$  and  $\gamma_{lv}^d$  refer to the polar and dispersive components of the solvent SFE, respectively. The polar and dispersive components of the solid are respectively the squares of slope and intercept of the equation above. Given that OWRK equation has two unknowns, this model necessitates using at least two solvents with known polar and dispersive tensions  $\gamma_{lv}^d$  and  $\gamma_{lv}^p$ .

### 3.1.3. Polar and disperse components of the SFE

The measured contact angles (Figure 2) and the polar and disperse components of the surface tension of the solvents (Table 1) were introduced in OWKR model. The elaboration of this model for different durations of UV/ozone treatments is presented in Figure 3. This figure also shows the approximate linear trendlines and their corresponding equations and correlation coefficients ( $R^2$ ). It is observed that almost all the correlation coefficients exceed 0.95, which demonstrates the

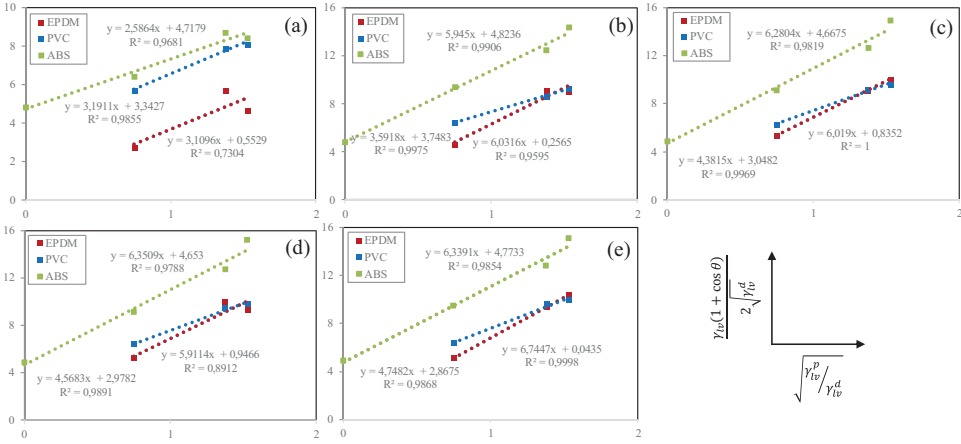


**Figure 3.** OWKR elaboration of samples treated for (a) 0 min, (b) 3 min, (c) 5 min, (d) 7 min, and (e) 10 min.

accuracy of the trendlines in approximating the experimental data. These trendlines will be used to determine the SFE of the model systems. As highlighted in Equation (4), the SFE is the sum of the polar and disperse components, given as the squares of the slope and intercept of OWKR trendlines, respectively, as shown in Equation (5).

Figure 4 presents the SFE polar and disperse components of the studied materials for different durations of UV/ozone treatment. Figure 4a shows that untreated EPDM initially has low SFE. After UV/ozone treatment, its polar component increased significantly while its disperse component remained negligible. The total surface energy of EPDM is in agreement with previous studies.<sup>[41]</sup> The contribution of the polar and disperse components depends on many parameters like surface treatment, aging, composition (e.g., content % of AN in ABS material, additives, etc.).<sup>[41]</sup> Figure 4b,c shows that untreated PVC and ABS have higher SFE than untreated EPDM, mainly due to the higher disperse components. After UV/ozone treatment, their SFEs increased significantly, mostly due to the increase of their polar components. Their disperse components are only slightly affected by the treatment. These results confirm previous findings showing that UV/ozone treatment affects mostly the polar component of the SFE.<sup>[4,13,42]</sup> Furthermore, it is observed that, after 3 min of treatment, the polar component increased significantly on EPDM and ABS surfaces compared to PVC. This increase becomes less significant at higher treatment durations. Similar observations were previously made for the contact angle measurements (Figure 2). This may suggest that the contact angle of the examined materials is more associated with the polar part of the SFE.

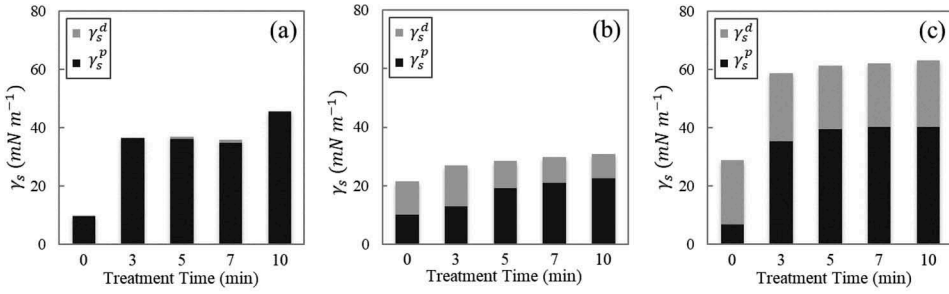


**Figure 4.** Effect of UV/ozone treatment on the SFE polar and disperse components obtained using OWKR model (a) EPDM, (b) PVC, and (c) ABS.

### 3.1.4. Wetting envelopes (WE)

The wetting behavior is best characterized using the wetting envelopes. These envelopes can be used to determine the wettability of other solvents, with known polar and disperse components, without conducting contact angle measurements. The envelopes are obtained using OWRK equation by expressing  $\gamma_{lv}^p$  in terms of  $\gamma_{lv}^d$  as follows<sup>[43]</sup>:

$$\left[ \frac{(1 + \cos \theta)}{2} \right] \gamma_{lv}^p - \left[ \sqrt{\gamma_s^p} \right] \sqrt{\gamma_{lv}^p} = \left[ -\frac{(1 + \cos \theta)}{2} \right] \gamma_{lv}^d + \left[ \sqrt{\gamma_s^d} \right] \sqrt{\gamma_{lv}^d} \quad (6)$$

In Equation (6), the polar component of the solvent surface tension ( $\gamma_{lv}^p$ ) is expressed in terms of the disperse component ( $\gamma_{lv}^d$ ), and those of the material ( $\gamma_s^p$  and  $\gamma_s^d$ ) are used as coefficients. This relationship can be drawn as a wetting envelope. The contact angle ( $\theta$ ) can be changed to obtain the corresponding envelope. The wetting envelope of each solid is used to determine the wettability of any solvent whose dispersive and polar components are used as coordinates.

The wetting envelopes of untreated EPDM, PVC, and ABS are presented in Figure 5. The figure shows the contours of different contact angles including  $\theta = 0^\circ$  which corresponds to complete wetting. The coordinate axes of these plots correspond to the polar and disperse components of the solvent surface tension. To verify the accuracy of the envelopes, the points corresponding to the solvents used in this analysis (i.e., water, ethylene glycol-water, and glycerol) are located in the graphs. The coordinates of these points are the polar and disperse components presented in Table 1. The contact angles obtained using these solvents are shown in brackets. An extra contour of  $\theta = 120^\circ$  is plotted for EPDM due to the high contact angles obtained for this material. It is clearly observed that the positions of the three solvents are consistent with the wetting envelopes. Their contact angles are ordered and well positioned between the envelopes that correspond to lower and higher contact angles. This result was obtained for the three materials. Therefore, OWRK model effectively characterizes the wettability of the samples, and the envelopes can be reliably used to predict the wettability of the materials by other solvents.

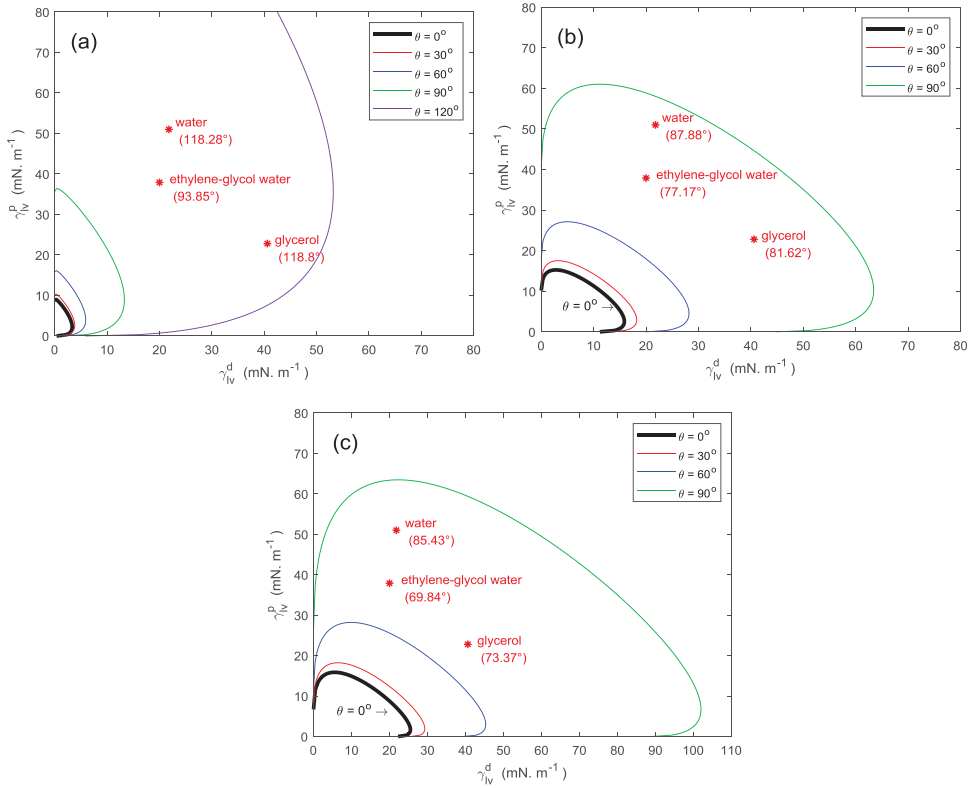


**Figure 5.** Wetting envelopes of untreated (a) EPDM, (b) PVC, and (c) ABS with  $0^\circ$ ,  $30^\circ$ ,  $60^\circ$ ,  $90^\circ$ , and  $120^\circ$  contours.

Unlike the current study, several previous studies found discrepancies in their wetting envelopes.<sup>[21,40,43]</sup> In these studies, the plotted points corresponding to the used solvents were not located between the right envelopes. This may indicate that Fowkes' assumptions considered in OWRK model, such as the comparability of the distance between the interacting volume elements, are not fully satisfied.<sup>[43]</sup>

It is observed in Figure 5 that, for each contact angle  $\theta$ , the wetting envelopes of PVC and ABS are much wider than that of EPDM. For instance, for  $\theta = 30^\circ$  (blue curves), the area enclosed within the envelope of EPDM (Figure 5a) is much narrower than those enclosed by the envelopes of PVC (Figure 5b) and ABS (Figure 5c). To better highlight this point, the wetting envelopes of the three materials in the case of complete wetting ( $\theta = 0^\circ$ ) are plotted in the same graph in Figure 6. This figure clearly shows that PVC and ABS envelopes enclose a much larger area and thus include higher ranges of surface tension compared to EPDM. Therefore, these two materials have a much higher wettability.

To have a better understanding on the effect of UV/ozone treatment on wettability, Figure 7 presents the wetting envelopes of the materials for  $\theta = 60^\circ$  at treatment durations of 0 min (UV0), 3 min (UV3), and 10 min

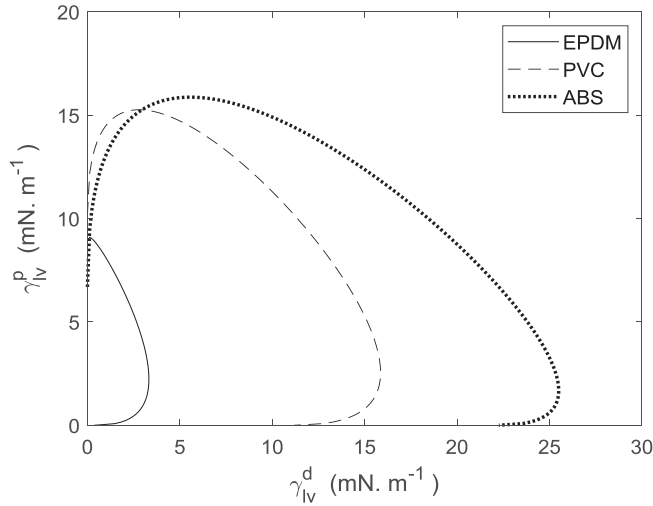


**Figure 6.** Wetting envelopes of the model systems at a complete wetting ( $\theta = 0^\circ$ ).

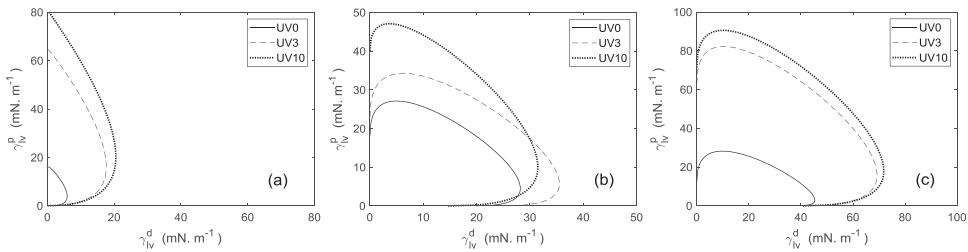


**Figure 7.** Effect of UV/ozone treatment on the wetting envelopes of (a) EPDM, (b) PVC, and (c) ABS for  $\theta = 60^\circ$ .

(UV10). These results are also representative of the other contact angles. It is clearly shown that UV/ozone treatment increases the area enclosed by the wetting envelopes. Therefore, solvents that initially did not wet the materials, thus fell outside the envelopes, will wet them after the treatment. This is particularly significant in the case of ABS. However, the envelope of EPDM expanded mostly in the polar direction after treatment, which makes the enclosed area less wide and the possibility of being wet by new solvents less likely to occur (Figure 7a). These results show the improvement in wettability after UV/ozone treatment, which is consistent with a previous study on PE and PEEK.<sup>[3]</sup>

### 3.2. Adhesion analysis

Figure 8 highlights the T-peel strength of EPDM and PVC, and the lap-shear strength of ABS before and after UV/ozone treatment. The adhesive strength

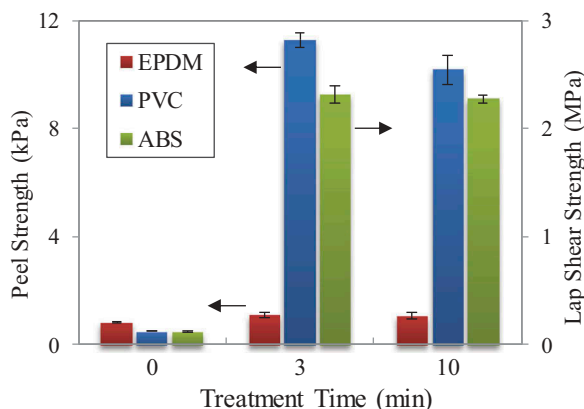


**Figure 8.** Effect of UV/ozone treatment on the lap-shear strength of ABS and T-peel strength of EPDM and PVC.

of all the materials is initially low. After treating the samples for 3 min, no significant change is observed for EPDM, while the strength of PVC and ABS increased significantly. After 10 min of treatment, the adhesive strength of EPDM is still low, while that of PVC and ABS stayed high. These results clearly demonstrate that 3 min of UV/ozone treatment are sufficient to improve the adhesive bond strength of PVC and ABS.

However, UV/ozone treatment changed not only the adhesive strength of the examined materials, but more importantly, their failure mechanisms. [Figure 9](#) shows the failure modes of the samples before and after 3 min of treatment. White dashed lines were added to indicate the bondlines between black EPDM samples and the black adhesive. The bondlines are shown on the left-hand side of the lines. EPDM fails adhesively before and after UV/ozone treatment. This shows that the treatment did not sufficiently improve the EPDM-adhesive interface. However, the failure modes of PVC and ABS changed from adhesive to cohesive after UV/ozone treatment. This highlights a significant improvement in the interface quality. Thus, the improvement of the bonding strength of PVC and ABS after treatment is accompanied with a shift in their failure modes from adhesive to cohesive.

By comparing the adhesion and wettability results, it is observed that EPDM has low adhesion strength after UV/ozone treatment ([Figure 8](#)) despite its high SFE polar component ([Figure 4](#)). Previous studies mistakenly made a straightforward correlation between the adhesion strength and the polar component of the SFE. For example, Cirilin and Kaelble claimed that the shear bond strength of stretched Teflon increased with higher surface fractional polarity.<sup>[15]</sup> However, their results presented in Tables II, III, and IV of their paper demonstrate that higher fractional polarity does not always correspond to a higher work of adhesion.<sup>[15]</sup> This can be explained by the

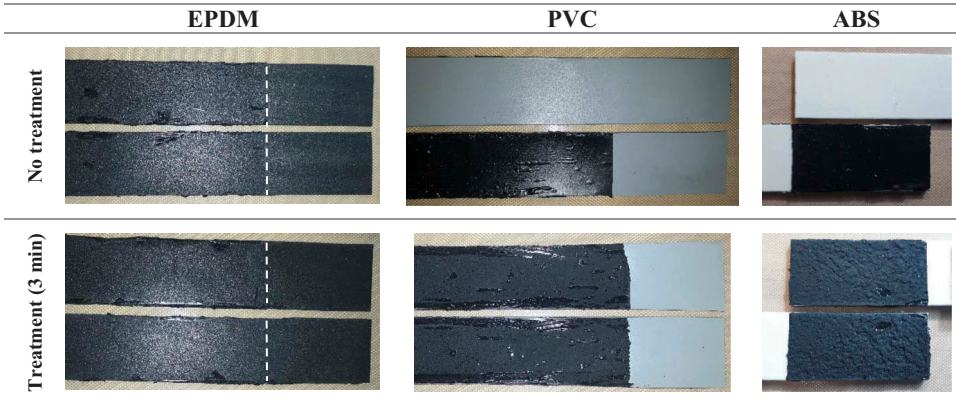


**Figure 9.** Effect of UV/ozone treatment on the failure modes of the bonded joints.

Good-Fowkes equation which expresses the work of adhesion ( $W_a$ ) as the sum of a polar ( $p$ ) and a disperse ( $d$ ) components<sup>[15]</sup>:

$$W_a = W_a^d + W_a^p \quad (7)$$

Therefore, the disperse component of the material also plays a role in its adhesive strength. Previous studies introduced a more reliable parameter that relates wettability to the mechanical strength of adhesion, namely the *work of spreading* ( $W_s$ ).<sup>[17,44]</sup> This thermodynamic quantity, defined as the difference between the work of adhesion and the work of cohesion ( $W_c$ ), will be considered in future studies:

$$W_s = W_a - W_c \quad (8)$$

Furthermore, it is observed that EPDM still has a low adhesive strength after UV/ozone treatment (Figure 8) although its wetting curve became much wider after treatment (Figure 7a). Previous studies correlated adhesive strength to wettability of adhesives. For instance, Gledhill and co-workers studied the butt joint strength of steel cylinders bonded with an epoxide adhesive. They found that higher strength is associated with higher wettability reflected by more expanded wetting envelopes.<sup>[40]</sup> However, the wetting of surfaces by adhesives is a necessary, though sometimes insufficient, requirement to develop joints with strong adhesion.<sup>[19]</sup> A previous study found that abrasion treatment caused lower wettability yet higher adhesion strength of UHMWPE surfaces.<sup>[5]</sup> To assure good adhesive bonding, other physical and/or chemical mechanisms, such as mechanical interlocking, should take place to make the spreading of the adhesive across the surface (i.e., wettability) more efficient. Similarly, the direct correlation between the bonding strength and the surface energy is misleading. A previous study found that air plasma treatment leads to higher surface tension but lower adhesion strength compared to nitrogen plasma treatment.<sup>[45]</sup>



Therefore, it is crucial to have a deeper insight into the mechanisms that lead to the improvement of the wettability and adhesion of PVC and ABS materials. This can be achieved by investigating the impact of UV/ozone treatment on the chemical structures and morphological features of their surfaces.

### 3.3. Chemical and morphological analysis

#### 3.3.1. Surface chemical structure

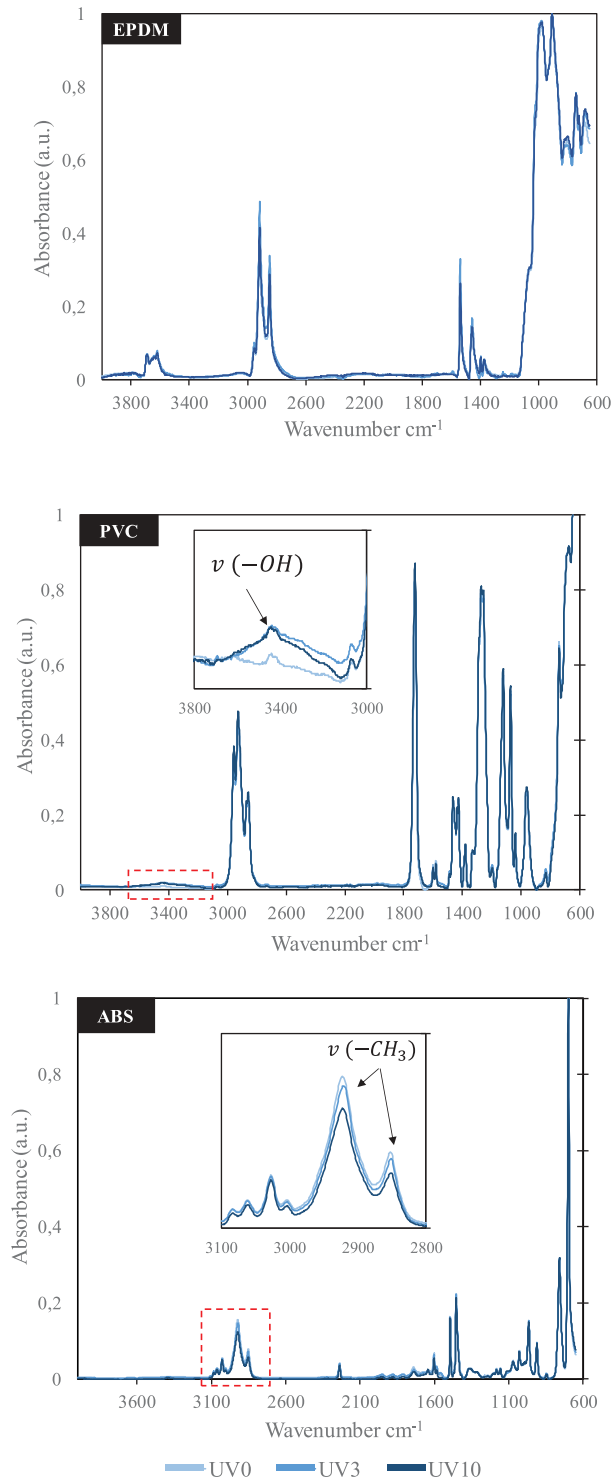
FTIR spectra were collected to investigate the impact of UV/ozone treatment on the structures of the model systems. The results were first pre-processed by correcting the baseline and the offset and normalizing the spectra using min-max normalization method.<sup>[38]</sup> Figure 10 shows the FTIR spectra of the studied materials without UV/ozone treatment (UV0) and after 3 min (UV3) and 10 min (UV10) of treatment. The vibrational modes of the chemical groups are also indicated in the figure.<sup>[17]</sup> It is clearly shown that the treatment effect on EPDM spectra is insignificant. This can be explained by either its chemical stability or the effectiveness of the added fillers such as light stabilizers and carbon black. Similarly, PVC spectra changed slightly after UV/ozone treatment. An insignificant increase is observed at the absorbance band of  $3100\text{--}3500\text{ cm}^{-1}$ , which corresponds to the stretching of the hydroxyl region ( $\text{--OH}$ ).<sup>[46,47]</sup> This band can be associated with one of the PVC fillers, like the hydroxides frequently used as flame retardants (e.g., ATH aluminum hydroxide).<sup>[48]</sup> Likewise, the treatment-induced change in ABS spectra is insignificant. Only the peaks within the absorbance bands of  $2800\text{--}3100\text{ cm}^{-1}$  were slightly attenuated. These bands are associated with the stretching mode of  $\text{C--H}$  groups.<sup>[46,47]</sup>

The FTIR analysis shows that UV/ozone treatment caused insignificant changes in the chemical structures of the studied materials. A better understanding will be gained by investigating the effect of this treatment on their surface morphology using microscopic observations.<sup>[49,50]</sup>

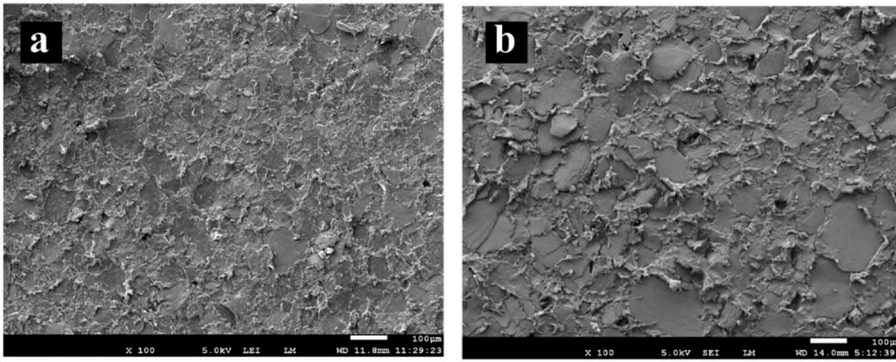
#### 3.3.2. Surface morphology

Figure 11 presents the SEM micrographs of untreated and 10 min treated EPDM surfaces. After treatment, the surface is cleaner and the plate-like microstructures are better observed. This cleaning process occurs when the photons of UV irradiation interact first with oxygen to form ozone; then, with ozone to produce atomic oxygen radicals. Both ozone and atomic oxygen radicals can react with the polymer surfaces to remove low-weight contaminants.<sup>[12,13,51]</sup> However, no new microstructures are observed on EPDM surfaces after UV/ozone treatment.

Likewise, the effect of 10 min of UV/ozone treatment on the morphology of PVC surfaces is shown in Figure 12. Initially, small ruffles are observed on untreated surfaces, indicating the presence of surface impurities (Figure 12a). These particles were removed after the treatment, making the surface much



**Figure 10.** FTIR-ATR spectra of untreated and treated samples.  $\nu$  = stretching vibrational mode.



**Figure 11.** SEM micrographs of EPDM surfaces (a) untreated (b) treated for 10 minutes.

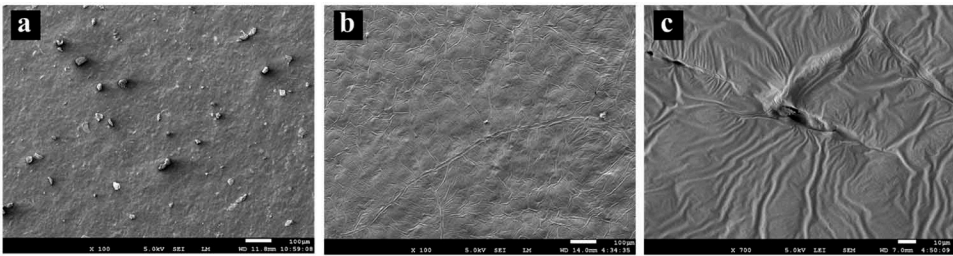


**Figure 12.** SEM micrographs of PVC surfaces (a) untreated (b, c) treated for 10 min.

cleaner. Also, a network of small wrinkles is observed on the treated surface, significantly changing their morphology (Figure 12b,c). Figure 12c also shows that some wrinkles were developed into microholes indicating the violent degradation onset of one of the material inorganic additives.<sup>[52]</sup> Other SEM observations showed that these microholes increase in size and number with higher durations of UV/ozone treatment.

Similarly, Figure 13 compares untreated ABS surfaces with those treated for 10 min. It clearly shows the creation of micro-pores with a diameter of approximately  $0.1\ \mu\text{m}$  after UV/ozone treatment. This porous structure is observed on the whole-treated surface. Also, other SEM observations showed that the size of the pores increases with higher treatment duration.

The morphological changes observed in the SEM micrographs might explain the improvement of the adhesion strength after UV/ozone treatment. Figures 8 and 9 showed that the adhesive bond strength of PVC increased significantly after treatment and the failure mode shifted from adhesive to cohesive. This can be explained by the removal of surface impurities and the creation of wrinkles and micro-holes due to UV/ozone treatment (Figure 12b,c). These new features promote more efficient mechanical interlocking between the adhesive and the material, thus improve the adhesion strength.<sup>[53]</sup> Likewise, the porous structure of treated ABS surface (Figure 13) enhances its mechanical interlocking and

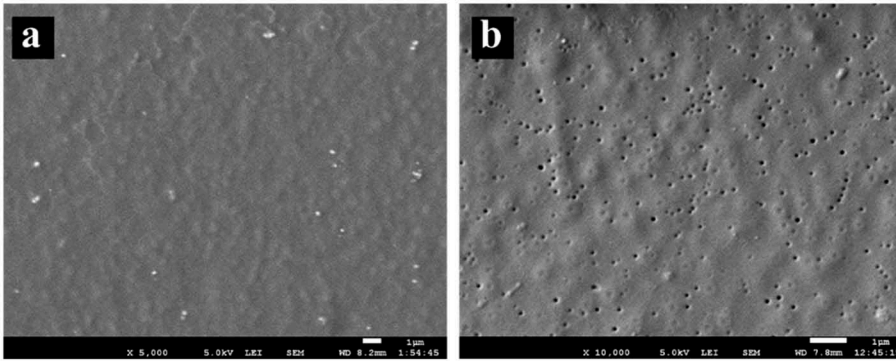


**Figure 13.** SEM micrographs of ABS surfaces (a) untreated (b) treated for 10 min.

adhesive strength (Figures 8 and 9). Similar effects were previously observed on metallic surfaces.<sup>[54]</sup> Their structure became micro-porous after etching and anodization treatments and their adhesive bonding strength increased. The lack of considerable improvement in the adhesion of EPDM after UV/ozone treatment is partly explained by the absence of new surface features (Figure 11).

The results presented in this study suggest that UV/ozone treatment affects primarily the morphological features of the examined surfaces, not their chemical structures. This observation is aligned with previous studies from the literature. Brewis and Briggs previously argued that the topographical function of UV/ozone treatment is the essential one, and its chemical function is just secondary.<sup>[4]</sup> Therefore, the improvement in the adhesion strength is mainly caused by the topographical effect of the UV/ozone treatment.

The results presented in this study can be used to make polymeric surfaces with higher adhesion strength. By simply exposing these surfaces to UV/ozone radiation, a significant improvement can be obtained in their adhesion behavior. This treatment can be easily implemented in the manufacturing process of polymeric products. Its efficiency can be improved by increasing the ozone concentration using oxygen concentrator, fan, or air pump. To complement this analysis, the effect and mechanisms of other surface treatments will be investigated in the future.

#### 4. Conclusion

The effect of UV/ozone treatment on the wettability and adhesion of EPDM, PVC, and ABS surfaces was investigated. It is found that the SFE and wettability improved after treatment, especially for PVC and ABS materials. OWKR wettability model showed that the SFE increased mainly due to the increase of its polar component. The wetting envelopes of the studied materials became wider after treatment, reflecting higher wettability. The adhesive bond strength of flexible bonded EPDM and PVC joints and hard ABS joints were investigated by

conducting T-peel test according to ASTM D1876 standard and lap-shear test according to ASTM D3163 standard, respectively. Results show that, after UV/ozone treatment, the adhesive bond strength of EPDM did not change significantly and its failure mode remained 100% adhesive (i.e., on the EPDM interface). However, the adhesive bond strength of PVC and ABS joints improved considerably and their failure modes changed from 100% adhesive to 100% cohesive (i.e., inside the adhesive). To better understand the mechanisms that lead to this adhesion improvement, FTIR-ATR characterization and SEM observations were performed on untreated and 10 min treated surfaces. The FTIR-ATR characterization showed insignificant changes in the chemical composition of the studied materials after UV/ozone treatment. However, SEM observations showed the creation of new wrinkles and micro-holes on treated PVC surfaces. Similarly, ABS surface became porous after UV/ozone treatment. No similar treatment-induced morphological features were observed on EPDM surfaces. These topographical changes might increase the surface area and enhance the mechanical interlocking between the adherends and the applied adhesive, thus improve their adhesive bond strength. This study opens new avenues for more straightforward and effective surface treatments that can be used to improve the wettability and adhesive bond strength of polymeric surfaces. Other treatments are being investigated and will be presented in the future.

## Acknowledgements

The authors would like specially thank Frans Oostrum from the Delft Aerospace Structures and Materials Laboratory (DASML) at the Faculty of Aerospace Engineering of Delft University of Technology for his insight and assistance.

## Funding

The authors would like to acknowledge the generous financial support of the project partners and the Rijksdienst voor ondernemend Nederland (the Netherlands Enterprise Agency).

## ORCID

Marouen Hamdi  <http://orcid.org/0000-0001-8615-9896>

Johannes A. Poulis  <http://orcid.org/0000-0003-3041-5285>

## References

- [1] Hamdi, M.; 2016. Fundamental Understanding of Scratch and Mar Behavior of Polymers. Dr. Diss., Texas A M Univ.
- [2] Chrisman, J.; Xiao, S.; Hamdi, M.; Pham, H.; Mullins, M. J.; Sue, H.-J. Testing and Evaluation of Mar Visibility Resistance for Polymer Films. *Polym. Test.* 2018, 69, 238–244. DOI: 10.1016/j.polymertesting.2018.05.011.

- [3] Mathieson, I.; Bradley, R. H. Improved Adhesion to Polymers by UV/ozone Surface Oxidation. *Int. J. Adhes. Adhes.* **1996**, *16*(1), 29–31. DOI: [10.1016/0143-7496\(96\)88482-X](https://doi.org/10.1016/0143-7496(96)88482-X).
- [4] Brewis, D. M.; Briggs, D. Adhesion to Polyethylene and Polypropylene. *Polymer (Guildf)* **1981**Jan, *22*(1), 7–16. DOI: [10.1016/0032-3861\(81\)90068-9](https://doi.org/10.1016/0032-3861(81)90068-9).
- [5] Oosterom, R.; Ahmed, T. J.; Poulis, J. A.; Bersee, H. E. N. Adhesion Performance of UHMWPE after Different Surface Modification Techniques. *Med. Eng. Phys.* **2006**May, *28*(4), 323–330. DOI: [10.1016/j.medengphy.2005.07.009](https://doi.org/10.1016/j.medengphy.2005.07.009).
- [6] Encinas, N.; Abenojar, J.; Martínez, M. A. Development of Improved Polypropylene Adhesive Bonding by Abrasion and Atmospheric Plasma Surface Modifications. *Int. J. Adhes. Adhes.* **2012**Mar, *33*, 1–6. DOI: [10.1016/j.ijadhadh.2011.10.002](https://doi.org/10.1016/j.ijadhadh.2011.10.002).
- [7] Encinas, N.; Díaz-Benito, B.; Abenojar, J.; Martínez, M. A. Extreme Durability of Wettability Changes on Polyolefin Surfaces by Atmospheric Pressure Plasma Torch. *Surf. Coatings Technol.* **2010**Oct, *205*(2), 396–402. DOI: [10.1016/j.surfcoat.2010.06.069](https://doi.org/10.1016/j.surfcoat.2010.06.069).
- [8] Abenojar, J.; Martínez, M. A.; Encinas, N.; Velasco, F. Modification of Glass Surfaces Adhesion Properties by Atmospheric Pressure Plasma Torch. *Int. J. Adhes. Adhes.* **2013**, *44*, 1–8. DOI: [10.1016/j.ijadhadh.2013.02.002](https://doi.org/10.1016/j.ijadhadh.2013.02.002).
- [9] Encinas, N.; Dillingham, R. G.; Oakley, B. R.; Abenojar, J.; Martínez, M. A.; Pantoja, M. Atmospheric Pressure Plasma Hydrophilic Modification of a Silicone Surface. *J. Adhes.* **2012**, *88*(4–6), 321–336. DOI: [10.1080/00218464.2012.659994](https://doi.org/10.1080/00218464.2012.659994).
- [10] Rodríguez-Villanueva, C.; Encinas, N.; Abenojar, J.; Martínez, M. A. Assessment of Atmospheric Plasma Treatment Cleaning Effect on Steel Surfaces. *Surf. Coatings Technol.* **2013**Dec, *236*, 450–456. DOI: [10.1016/j.surfcoat.2013.10.036](https://doi.org/10.1016/j.surfcoat.2013.10.036).
- [11] Kupski, J.; Teixeira de Freitas, S.; Zarouchas, D.; Camanho, P. P.; Benedictus, R. Composite Layup Effect on the Failure Mechanism of Single Lap Bonded Joints. *Compos. Struct.* **2019**Jun, *217*, 14–26. DOI: [10.1016/j.compstruct.2019.02.093](https://doi.org/10.1016/j.compstruct.2019.02.093).
- [12] Peeling, J.; Clark, D. T. Surface Ozonation and Photooxidation of Polyethylene Film. *J. Polym. Sci. Polym. Chem. Ed.* **1983**Jul, *21*(7), 2047–2055. DOI: [10.1002/pol.1983.170210715](https://doi.org/10.1002/pol.1983.170210715).
- [13] Landete-Ruiz, M. D.; Martín-Martínez, J. M. Surface Modification of EVA Copolymer by UV Treatment. *Int. J. Adhes. Adhes.* **2005**Apr, *25*(2), 139–145. DOI: [10.1016/j.ijadhadh.2004.06.001](https://doi.org/10.1016/j.ijadhadh.2004.06.001).
- [14] Janssen, D.; De Palma, R.; Verlaak, S.; Heremans, P.; Dehaen, W. Static Solvent Contact Angle Measurements, Surface Free Energy and Wettability Determination of Various Self-assembled Monolayers on Silicon Dioxide. *Thin Solid Films* **2006**Dec, *515*(4), 1433–1438. DOI: [10.1016/j.tsf.2006.04.006](https://doi.org/10.1016/j.tsf.2006.04.006).
- [15] Cirlin, E. H.; Kaelble, D. H. Roughness and Anisotropy Effects on Wettability of Polytetrafluoroethylene and Sodium-treated Polytetrafluoroethylene. *J. Polym. Sci. Part A-2 Polym. Phys.* **1973**Apr, *11*(4), 785–799. DOI: [10.1002/pol.1973.180110411](https://doi.org/10.1002/pol.1973.180110411).
- [16] Encinas, N.; Pantoja, M.; Torres-Remiro, M.; Martínez, M. A. Approaches to poly-(tetrafluoroethylene) Adhesive Bonding. *J. Adhes.* **2011**Jul, *87*(7–8), 709–719. DOI: [10.1080/00218464.2011.596778](https://doi.org/10.1080/00218464.2011.596778).
- [17] Ahmad, J.; Bazaka, K.; Oelgemöller, M.; Jacob, M. Wetting, Solubility and Chemical Characteristics of Plasma-Polymerized 1-isopropyl-4-methyl-1,4-cyclohexadiene Thin Films. *Coatings* **2014** Jul, *4*(3), 527–552. doi: [10.3390/coatings4030527](https://doi.org/10.3390/coatings4030527).
- [18] Abenojar, J.; Torregrosa-Coque, R.; Martínez, M. A.; Martín-Martínez, J. M. Surface Modifications of Polycarbonate (PC) and Acrylonitrile Butadiene Styrene (ABS) Copolymer by Treatment with Atmospheric Plasma. *Surf. Coatings Technol.* **2009**May, *203*(16), 2173–2180. DOI: [10.1016/j.surfcoat.2009.01.037](https://doi.org/10.1016/j.surfcoat.2009.01.037).
- [19] Owens, D. K.; Wendt, R. C. Estimation of the Surface Free Energy of Polymers. *J. Appl. Polym. Sci.* **1969**, *13*, 1741–1747. DOI: [10.1002/app.1969.070130815](https://doi.org/10.1002/app.1969.070130815).

- [20] Kaelble, D. H.; Dispersion-Polar Surface Tension Properties of Organic Solids. *J. Adhes.* **1970**, *2*(2), 66–81. DOI: [10.1080/0021846708544582](https://doi.org/10.1080/0021846708544582).
- [21] Tryznowski, M.; Izdebska-Podsiadły, J.; Żółek-Tryznowska, Z. Wettability and Surface Free Energy of NIPU Coatings Based on bis(2,3-dihydroxypropyl)ether Dicarboxylate. *Prog. Org. Coatings* **2017**Aug, *109*, 55–60. DOI: [10.1016/j.porgcoat.2017.04.011](https://doi.org/10.1016/j.porgcoat.2017.04.011).
- [22] Fox, H.; Zisman, W. The Spreading of Liquids on Low-energy Surfaces. II. Modified Tetrafluoroethylene Polymers. *J. Colloid Sci.* **1952**Apr, *7*(2), 109–121. DOI: [10.1016/0095-8522\(52\)90054-8](https://doi.org/10.1016/0095-8522(52)90054-8).
- [23] Fox, H.; Zisman, W. The Spreading of Liquids on Low-energy Surfaces. III. Hydrocarbon Surfaces. *J. Colloid Sci.* **1952**Aug, *7*(4), 428–442. DOI: [10.1016/0095-8522\(52\)90008-1](https://doi.org/10.1016/0095-8522(52)90008-1).
- [24] van Oss, C. J.; Chaudhury, M. K.; Good, R. J. Interfacial Lifshitz-van Der Waals and Polar Interactions in Macroscopic Systems. *Chem. Rev.* **1988**Sep, *88*(6), 927–941. DOI: [10.1021/cr00088a006](https://doi.org/10.1021/cr00088a006).
- [25] Neumann, A.; Good, R.; Hope, C.; Sejpal, M. An Equation-Of-state Approach to Determine Surface Tensions of Low-energy Solids from Contact Angles. *J. Colloid Interface Sci.* **1974**Nov, *49*(2), 291–304. DOI: [10.1016/0021-9797\(74\)90365-8](https://doi.org/10.1016/0021-9797(74)90365-8).
- [26] Hejda, F.; Solař, P.; Kousal, J. *Surface Free Energy Determination by Contact Angle Measurements-A Comparison of Various Approaches*. 2010, *10*,25-30.
- [27] Santos, R. M.; Botelho, G. L.; Cramez, C.; Machado, A. V. Outdoor and Accelerated Weathering of Acrylonitrile-butadiene-styrene: A Correlation Study. *Polym. Degrad. Stab.* **2013**, *98*(10), 2111–2115. DOI: [10.1016/j.polymdegradstab.2013.07.016](https://doi.org/10.1016/j.polymdegradstab.2013.07.016).
- [28] ASTM D2093. Standard Practice for Preparation of Surfaces of Plastics Prior to Adhesive Bonding. **2017**. DOI: [10.1520/D2093-03R17](https://doi.org/10.1520/D2093-03R17).
- [29] Jańczuk, B.; Białopiotrowicz, T.; Wójcik, W. The Components of Surface Tension of Liquids and Their Usefulness in Determinations of Surface Free Energy of Solids. *J. Colloid Interface Sci.* **1989**, *127*(1), 59–66. DOI: [10.1016/0021-9797\(89\)90007-6](https://doi.org/10.1016/0021-9797(89)90007-6).
- [30] Wu, S.; *Polymer Interface and Adhesion*; M. Dekker, New York, **1982**.
- [31] van Oss, C.; *Interfacial Forces in Aqueous Media, Second Edition*; CRC Press, Boca Raton, **2006**.
- [32] Kozowyk, P. R. B.; Poulis, J. A.; Langejans, G. H. J. Laboratory Strength Testing of Pine Wood and Birch Bark Adhesives: A First Study of the Material Properties of Pitch. *J. Archaeol. Sci. Reports* **2017**Jun, *13*, 49–59. DOI: [10.1016/j.jasrep.2017.03.006](https://doi.org/10.1016/j.jasrep.2017.03.006).
- [33] Severijns, C.; de Freitas, S. T.; Poulis, J. A. Susceptor-assisted Induction Curing Behaviour of a Two Component Epoxy Paste Adhesive for Aerospace Applications. *Int. J. Adhes. Adhes.* **2017**Jun, *75*, 155–164. DOI: [10.1016/j.ijadhadh.2017.03.005](https://doi.org/10.1016/j.ijadhadh.2017.03.005).
- [34] Kozowyk, P. R. B.; Langejans, G. H. J.; Poulis, J. A. Lap Shear and Impact Testing of Ochre and Beeswax in Experimental Middle Stone Age Compound Adhesives. *PLoS One* **2016**Mar, *11*(3), e0150436. DOI: [10.1371/journal.pone.0150436](https://doi.org/10.1371/journal.pone.0150436).
- [35] ASTM D3167-10. ASTM D 1876 – 01 Standard Test Method for Peel Resistance of Adhesives (T-peel test). West Conshohocken, PA; ASTM International, **2015**, *03*, 1–6.
- [36] ASTM Standards. *ASTM D3163—01 Standard Test Method for Determining Strength of Adhesively Bonded Rigid Plastic Lap-Shear Joints in Shear by Tension Loading*, West Conshohocken, PA; ASTM International, **2014**.
- [37] Hamdi, M.; Sue, H.-J. Effect of Color, Gloss, and Surface Texture Perception on Scratch and Mar Visibility in Polymers. *Mater. Des.* **2015**, *83*, 528–535. DOI: [10.1016/j.matdes.2015.06.073](https://doi.org/10.1016/j.matdes.2015.06.073).
- [38] Lasch, P.; Spectral Pre-processing for Biomedical Vibrational Spectroscopy and Microspectroscopic Imaging. *Chemom. Intell. Lab. Syst.* **2012**Aug, *117*, 100–114. DOI: [10.1016/j.chemolab.2012.03.011](https://doi.org/10.1016/j.chemolab.2012.03.011).

- [39] Hofmann, H. E.; Evaporation Rates of Organic Liquids. *Ind. Eng. Chem.* 1932Feb, 24 (2), 135–140. DOI: [10.1021/ie50266a004](https://doi.org/10.1021/ie50266a004).
- [40] Gledhill, R. A.; Kinloch, A. J.; Shaw, S. J. Effect of Relative Humidity on the Wettability of Steel Surfaces. *J. Adhes.* 1977Jan, 9(1), 81–85. DOI: [10.1080/00218467708075101](https://doi.org/10.1080/00218467708075101).
- [41] Bhowmick, A. K.; Konar, J.; Kole, S.; Narayanan, S. Surface Properties of EPDM, Silicone Rubber, and Their Blend during Aging. *J. Appl. Polym. Sci.* 1995, 57(5), 631–637. DOI: [10.1002/app.1995.070570513](https://doi.org/10.1002/app.1995.070570513).
- [42] Kinloch, A. J.; Surface Analysis and Pretreatment of Plastics and Metals. D. M. Brewis (Editor). Applied Science, London 1982, £24, ISBN 0-35334-992-4, Pp 268 + Xvi. *Surf. Interface Anal.* 1982Dec, 4(6), ii–ii. DOI: [10.1002/sia.v4.6](https://doi.org/10.1002/sia.v4.6).
- [43] Cappelletti, G.; Ardizzone, S.; Meroni, D.; Soliveri, G.; Ceotto, M.; Biaggi, C.; Benaglia, M.; Raimondi, L. Wettability of Bare and Fluorinated Silanes: A Combined Approach Based on Surface Free Energy Evaluations and Dipole Moment Calculations. *J. Colloid Interface Sci.* 2013, 389(1), 284–291.
- [44] Pogorzelski, S. J.; Rochowski, P.; Szurkowski, J. Pinus Sylvestris L. Needle Surface Wettability Parameters as Indicators of Atmospheric Environment Pollution Impacts: Novel Contact Angle Hysteresis Methodology. *Appl. Surf. Sci.* 2014Feb, 292, 857–866. DOI: [10.1016/j.apsusc.2013.12.062](https://doi.org/10.1016/j.apsusc.2013.12.062).
- [45] Noeske, M.; Degenhardt, J.; Strudthoff, S.; Lommatzsch, U. Plasma Jet Treatment of Five Polymers at Atmospheric Pressure: Surface Modifications and the Relevance for Adhesion. *Int. J. Adhes. Adhes.* 2004Apr, 24(2), 171–177. DOI: [10.1016/j.ijadhadh.2003.09.006](https://doi.org/10.1016/j.ijadhadh.2003.09.006).
- [46] Lambert, B. J.; Shurvell, D. A.; Lightner, F. H.; Cooks, R. G. *Introduction to Organic Spectroscopy*; New York: Macmillan, 1987.
- [47] Munajad, A.; Subroto, C.; Suwarno. Fourier Transform Infrared (FTIR) Spectroscopy Analysis of Transformer Paper in Mineral Oil-Paper Composite Insulation under Accelerated Thermal Aging. *Energies* 2018 Feb, 11(2), 364.
- [48] Pagacz, J.; Chrzanowski, M.; Krucińska, I.; Pielichowski, K. Thermal Aging and Accelerated Weathering of PVC/MMT Nanocomposites: Structural and Morphological Studies. *J. Appl. Polym. Sci.* 2015 Jun, 132(24). doi: [10.1002/app.v132.24](https://doi.org/10.1002/app.v132.24).
- [49] Lei, F. et al. Scratch Behavior of Epoxy Coating Containing Self-assembled Zirconium Phosphate Smectic Layers. *Polym. (United Kingdom)*. 2017, 112, 252–263.
- [50] Hamdi, M.; Zhang, X.; Sue, H.-J. Fundamental Understanding on Scratch Behavior of Polymeric Laminates. *Wear*. 2017, 380–381, 203–216. DOI: [10.1016/j.wear.2017.03.024](https://doi.org/10.1016/j.wear.2017.03.024).
- [51] Walzak, M. J.; Flynn, S.; Foerch, R.; Hill, J. M.; Karbasheski, E.; Lin, A.; Strobel, M. UV and Ozone Treatment of Polypropylene and poly(ethylene terephthalate). *J. Adhes. Sci. Technol.* 1995 Jan, 9(9), 1229–1248. doi: [10.1163/156856195X01012](https://doi.org/10.1163/156856195X01012).
- [52] Novis, Y.; De Meulemeester, R.; Chtaïb, M.; Pireaux, -J.-J.; Caudano, R. XPS and SEM Study of UV Laser Surface Modification of Polymers. *Br. Polym. J.* 1989Jan, 21(2), 147–153. DOI: [10.1002/\(ISSN\)1934-256X](https://doi.org/10.1002/(ISSN)1934-256X).
- [53] Pastor-Blas, M. M.; Sanchez-Adsuar, M. S.; Martin-Martinez, J. M. Surface Modification of Synthetic Vulcanized Rubber. *J. Adhes. Sci. Technol.* 1994Jan, 8(10), 1093–1114. DOI: [10.1163/156856194X00960](https://doi.org/10.1163/156856194X00960).
- [54] Venables, J. D.; Adhesion and Durability of Metal-polymer Bonds. *J. Mater. Sci.* 1984Aug, 19(8), 2431–2453. DOI: [10.1007/BF00557096](https://doi.org/10.1007/BF00557096).